Environmental and Experimental Botany 156 (2018) 96–105

Contents lists available at ScienceDirect

Environmental and Experimental Botany

journal homepage: www.elsevier.com/locate/envexpbot

Increased CO_2 exacerbates the stress of ultraviolet radiation on photosystem II function in the diatom *Thalassiosira weissflogii*

Guang Gao[a,c,1], Zhiguang Xu[a,1], Qi Shi[b], Hongyan Wu[a,b,*]

[a] College of Life Science, Ludong University, Yantai 264025, China
[b] Hubei University of Technology, Wuhan 430068, China
[c] Jiangsu Key Laboratory of Marine Resources and Environment, Huaihai Institute of Technology, Lianyungang 222005, China

ARTICLE INFO

Keywords:
Diatom
Ocean acidification
Photoinactivation
Photosystem II
Rubisco
Ultraviolet radiation

ABSTRACT

Diatoms usually dominate phytoplankton community in coastal waters and experience rapid changes of underwater light. However, little is known regarding how increased CO_2 would affect diatoms' capacity in dealing with changing photosynthetically active radiation (PAR) and ultraviolet radiation (UVR). Here, we cultured a globally abundant diatom *Thalassiosira weissflogii* under two levels of CO_2 (400, 1000 ppmv), and then analysed its PSII function during an increase in PAR and UVR to mimic an upward mixing event. UVR noticeably reduced photosystem II (PSII) activity (F_V/F_M) during the high light exposure, which was more significant for cells grown at the higher CO_2 condition. The PsbA removal rate (K_{PsbA}) was synergistically increased by high CO_2 and UVR, while the PsbD removal rate (K_{PsbD}) was decreased under higher CO_2. Both CO_2 and UVR had an inducible effect on sustained phase of nonphotochemical quenching (NPQs). The higher CO_2 decreased the ratio of Rubisco large subunit (RbcL) to PsbA regardless of the radiation treatments. It seems that the increased NPQs and turnover of PsbA induced by higher CO_2 were not enough to offset the stressful effect it brought about, particularly when higher CO_2 was combined with UVR. These findings indicate that increased CO_2 may exacerbate the harmful effect of UVR on PSII function in the *T. weissflogii* through reducing PsbD removal rate and the ratio of RbcL to PsbA during UVR exposure, and thus would affect its abundance and distribution in future ocean environment.

1. Introduction

Due largely to fossil fuel burning, the CO_2 level in atmosphere is continuously increasing. The oceans are a major sink for atmospheric CO_2 and thus mitigate the global change (Landschützer et al., 2015). However, continuous absorb of CO_2 leads to the decrease of pH in the oceans, termed ocean acidification. The pH in the surface ocean has decreased by 0.1 units since the beginning of the industrial era (Gattuso et al., 2015). According to the Representative Concentration Pathway (RCP) 8.5 projection, mean surface ocean pH will further decrease by 0.4 units by 2100 (Gattuso et al., 2015). The decline in seawater pH, together with the associated changes in seawater carbonate system, is affecting the whole marine ecosystem (Mostofa, 2016). In terms of phytoplankton, studies show that increased CO_2 could promote photosynthesis and growth in phytoplankton (Riebesell and Tortell, 2011; Mccarthy et al., 2012) or have no significant effects (Kim et al., 2006; Boelen et al., 2011) or even reduce CO_2 fixation (Gao et al., 2012; Mackey et al., 2015). The contrasting effects of increased CO_2 may be due to species difference and also the interaction with other environmental factors. For instance, increased CO_2 increases the effective photochemical efficiency and growth of three diatoms (*Phaeodactylum tricornutum*, *Thalassiosira pseudonana* and *Skeletonema costatum*) at lower solar radiation but reduced these physiological performances at higher solar radiation (Gao et al., 2012).

Solar ultraviolet radiation (UVR) is usually absorbed and screened by stratospheric ozone. However, depletion of ozone by industrial activities allows increased UVR to reach the earth's surface (Häder et al., 2007). Although stratospheric ozone depletion has been stalled and a recovery has been seen in the Antarctic Ozone Hole due to the effective implementation of the Montreal Protocol (Newman and Mckenzie, 2011; Solomon et al., 2016), chlorodifuoromethanes (HCFCs), the substitute for chlorinated fluorocarbons (CFCs), have a small but noticeable ozone depletion effect and their concentrations are rising (Wallington et al., 1994). It is presumed that UVR will decrease at mid and high latitudes (Bais et al., 2015), but the total ozone might be lower in the tropics compared to the 1960s (Panel, 2017). Accordingly, the

* Corresponding author at: College of Life Science, Ludong University, Yantai 264025, China.
E-mail address: sdwuhongyan@126.com (H. Wu).
[1] These authors contributed equallyto this work.

https://doi.org/10.1016/j.envexpbot.2018.08.031
Received 6 June 2018; Received in revised form 27 August 2018; Accepted 28 August 2018
Available online 30 August 2018
0098-8472/

Table 1
Parameters of the seawater carbonate system in two levels of CO_2 cultures. DIC = dissolved inorganic carbon, TA = total alkalinity. Data are the means ± SE (n = 4). Different superscript letters represent significant differences ($P < 0.05$) among cultures.

Air CO_2 (ppmv)	pCO_2 (μatm)	pH_{NBS}	DIC (μmol kg^{-1})	HCO_3^- (μmol kg^{-1})	CO_3^{2-} (μmol kg^{-1})	CO_2 (μmol kg^{-1})	TA (μmol kg^{-1})
400 ± 20	390 ± 10[a]	8.20 ± 0.01[b]	2151 ± 44[a]	1946 ± 39[a]	193 ± 5[b]	13.3 ± 0.3[a]	2432 ± 48[a]
1000 ± 50	987 ± 54[b]	7.85 ± 0.02[a]	2311 ± 50[b]	2182 ± 48[b]	96 ± 3[a]	33.7 ± 1.8[b]	2429 ± 48[a]

Table 2
Multivariate analysis of variance for the effects of CO_2 on pCO_2, pH, dissolved inorganic carbon (DIC), HCO_3^-, CO_3^{2-}, CO_2, total alkalinity (TA) in the seawater. df means degree of freedom, F means the value of F statistic, and Sig. means *p*-value.

Source		pCO_2		pH		DIC		HCO_3^-		CO_3^{2-}		CO_2		TA	
	df	F	Sig.	F	Sig.	F	Sig.	F	Sig.	F	Sig.	F	Sig.	F	Sig.
CO_2	1	474.276	< 0.001	1387.047	< 0.001	23.247	0.003	57.388	< 0.001	960.026	< 0.001	485.663	< 0.001	0.011	0.920
Error	6														

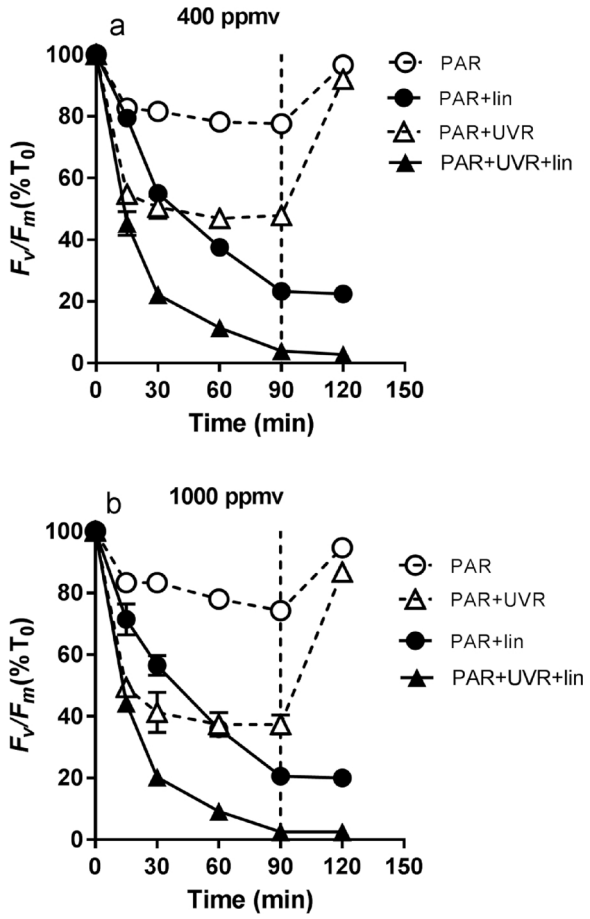

Fig. 1. Responses of PSII maximum photochemical yield (F_V/F_M) versus exposure time to high light in *T. weissflogii* cultures treated with (black symbols) or without (white symbols) the chloroplast protein synthesis inhibitor lincomycin. Cells were grown under two levels of CO_2 (400, 1000 ppmv) at the light intensity of 20 W m^{-2} PAR, then exposed to high radiation of PAR (140 W m^{-2}) or PAR (140 W m^{-2}) + UVR (26 W m^{-2}) for 90 min, and then allowed to recover at 20 W m^{-2} PAR for 30 min. The initial F_V/F_M was 0.688 ± 0.013 and 0.683 ± 0.014 for cells grown at 400 and 1000 ppmv CO_2 respectively. To analyse the effect of exposure time on F_V/F_M among different treatments, relative values (ratios of absolute to the initial values) were used here. Data are the means ± SE (n = 4), most error bars within symbols.

impacts of UVR on organisms have been gaining considerate attention (Häder et al., 2015). UVR could usually inhibit growth of phytoplankton (Gao et al., 2009; Domingues et al., 2017) through impairing the structure and function of DNA and proteins (Boelen et al., 2000; Gao et al., 2009) and the photosynthetic activity (Sobrino et al., 2008; Yin and Ulm, 2017).

Apart from the individual effect of increased CO_2 or UVR, the combined effects of them on phytoplankton have been also investigated. Wu et al. (2012b) reported that the relative electron transport rate in the diatom *Cylindrotheca closterium* f. *minutissima* was reduced by UVR which was more significantly for the cells cultured at elevated CO_2. Sobrino et al. (2009) also documented that elevated CO_2 levels enhanced sensitivity of phytoplankton in Lake Giles, Pennsylvania to UVR, leading to rising photoinhibition. However, the potential mechanisms of the interactive effect of CO_2 and UVR on PSII function in phytoplankton have yet to be fully understood.

Diatoms are cosmopolitan photosynthetic microalgae that can be found both in freshwater and oceans. Marine diatoms account for 75% of the primary productivity for coastal and nutrient-rich zones (Field et al., 1998; Falkowski, 2012), hence playing a vital role in the marine biological carbon pump as well as the biogeochemical cycling of nitrogen and silicon (Moore et al., 2013; Young and Morel, 2015). Marine diatoms are usually the dominating phytoplankton taxa in waters with vigorous mixing (Macintyre et al., 2000), where they have to address sudden increase of light exposure. Diatoms may experience transient excess light that can produce oxidative stress and thus cause damage to photosynthesis (Dubinsky et al., 2009; Wu et al., 2012a; Gao et al., 2018a). Diatoms have developed multiple strategies to increase their resilience to excess light. Cells can repair damaged PSII by replacing photo-damaged proteins in PSII with newly synthesized subunits (Nixon et al., 2010; Komenda et al., 2012). Compared to other marine phytoplankton taxa, marine diatoms have distinctive clearance patterns for the PsbA (D1), and PsbD (D2) PSII subunits and also a lower intrinsic susceptibility to photoinactivation of PSII upon elevated light levels (Six et al., 2009; Key et al., 2010; Mccarthy et al., 2012). Another important weapon of diatoms to deal with high light stress is non-photochemical quenching (NPQ) of captured excitation energy that is dominated by one or more mechanisms activated by the trans-thylakoid proton gradient triggering the xanthophyll cycle in diatoms (Lavaud et al., 2004; Lavaud and Lepetit, 2013). In addition, the fast run of Calvin cycle is also deemed to be an option for plants to drain off excess electrons by increasing consumption (Biehler, 1996; Li and Campbell, 2017).

Based on our previous studies (Gao et al., 2012, 2018a), we hypothesized that increased CO_2 would reduce diatoms' resilience to UVR and lead to synergistic photoinactivation of PSII for cells experiencing the treatments of increased CO_2 and UVR. In this study we cultured a globally abundant diatom *T. weissflogii* under two levels of CO_2 and then

Table 3
Repeated analysis of variance for the effects of exposure time on F_V/F_M, PsbA, PsbD and NPQs under various conditions. Time*CO_2 means the interactive effect of exposure time and CO_2 and the other terms with asterisk have similar meanings. df means degree of freedom, F means the value of F statistic, and Sig. means *p*-value.

Source	F_V/F_M			PsbA			PsbD			NPQs		
	df	F	Sig.	df	F	Sig.	df	F	Sig.	df	F	Sig.
Time	4	1397.279	< 0.001	4	88.253	< 0.001	4	120.137	< 0.001	4	288.347	< 0.001
Time*CO_2	4	1.619	0.176	4	2.128	0.087	4	1.395	0.246	4	1.990	0.102
Time*UVR	4	109.234	< 0.001	4	26.378	< 0.001	4	3.167	0.019	4	22.093	< 0.001
Time*lincom	4	205.876	< 0.001	4	27.680	< 0.001	4	12.118	< 0.001	4	53.434	< 0.001
Time*CO_2*UVR	4	1.450	0.224	4	1.578	0.191	4	1.258	0.296	4	1.241	0.299
Time* CO_2*lincom	4	1.098	0.362	4	0.745	0.565	4	1.303	0.278	4	0.418	0.795
Time* UVR*lincom	4	5.708	< 0.001	4	4.775	0.002	4	0.314	0.868	4	3.443	0.011
Time*CO_2*UVR*lincom	4	0.757	0.556	4	0.285	0.887	4	0.697	0.597	4	0.647	0.630
Error	96			64			64			96		

Table 4
Multivariate analysis of variance for the effects of CO_2, UVR and lincomycin on F_V/F_M and PsbA content at different time points. CO_2*UVR means the interactive effect of CO_2 and UVR and the other terms with asterisk have similar meanings. df means degree of freedom, F means the value of F statistic, and Sig. means *p*-value.

Source	F_V/F_M					PsbA				
	90 min			120 min		90 min			120 min	
	F	Sig.	df	F	Sig.	F	Sig.	df	F	Sig.
CO_2	13.699	0.001	1	9.526	0.005	7.468	0.015	1	0.073	0.790
UVR	461.475	< 0.001	1	237.313	< 0.001	124.417	< 0.001	1	14.523	0.002
Lincom	1489.371	< 0.001	1	9965.773	< 0.001	138.479	< 0.001	1	234.269	< 0.001
CO_2*UVR	1.553	0.225	1	0.092	0.764	0.796	0.385	1	1.832	0.195
CO_2*lincom	3.987	0.057	1	2.038	0.166	0.376	0.548	1	4.250	0.056
UVR*lincom	36.391	< 0.001	1	58.283	< 0.001	9.754	0.007	1	4.080	0.060
CO_2*UVR*lincom	3.019	0.095	1	2.719	0.112	< 0.001	1.000	1	0.878	0.363
Error			24					16		

exposed it to two radiation treatments (PAR, PAR + UVR) to test this hypothesis via studying the variation of PSII subunit turnover rate, NPQs, key proteins for Calvin cycle under different treatments.

2. Materials and methods

2.1. Experiment design

The diatom species, *Thalassiosira weissflogii* (CCMA102), was isolated from the Northern South China Sea. Cells were grown semi-continuously in artificial seawater (Morel et al., 1979) with the addition of f/2 medium (Guillard and Ryther, 1962). Two levels of CO_2 (400, 1000 ppmv) were controlled by CO_2 incubators (HP 1000G-D, Ruihua, China). The lower and higher CO_2 represent the current and the level by 2100 respectively (Gattuso et al., 2015). To make the seawater carbonate stable (pH variations < 0.05 units), the cultures were diluted by pre − CO_2-equilibrated medium every 24 h, and the cell density was maintained no more than 10 μg chlorophyll *a* L^{-1}. Cultures in the CO_2 incubators were illuminated by cool white fluorescent tubes with 20 W m^{-2} and a 12 h: 12 h (light: dark) cycle. To ensure full acclimation, all cultures were conducted at least seven transfers of semi-continuous dilution before use in the subsequent experiments. There were four replicates for each treatment.

2.2. Measurement of seawater carbonates parameters

The variation of pH in the medium was monitored using a pH meter (SevenMulti S40K, Mettler-Toledo). DIC was determined by a Shimadzu Total Organic Carbon Analyzer (TOC-5000A, Japan) and total alkalinity was measured by potentiomentric titration. Subsequently, other parameters of the carbonate system were calculated using a CO_2SYS software (Pierrot et al., 2006) based on the known values of temperature, salinity, pH, DIC and alkalinity.

2.3. Upward light shift and recovery experiment

Each culture was split into two quartz flasks. One quartz flask was supplemented with lincomycin with the final concentration of 500 μg mL^{-1} to block chloroplast protein synthesis (Gao et al., 2018a), thus inhibiting PSII repair (Tyystjärvi and Aro, 1996; Gao et al., 2018a) and the other one was kept as it was. Both flasks were placed in the dark for 10 min to allow the lincomycin to exert its effect and then exposed to a solar simulator (Sol 1200, Dr. Hönle GmbH, Germany). The cultures in quartz tubes received PAR + UVR (295–700 nm) by covering with Ultraphan film 295 (UV Opak, Digefra, Munich, Germany) and received only PAR (400–700 nm) by covering with Ultraphan film 395 (UV Opak, Digefra, Munich, Germany). The irradiances of PAR and UVR were 140 and 26 W m^{-2} respectively.

Samples were collected prior to the onset of high light treatment (plotted as time 0) and then after 15, 30, 60, and 90 min exposure for chlorophyll fluorescence analyses and also for protein immunoblotting. After the high-light treatment, the remaining cultures were returned to their growth light of 20 W m^{-2} PAR for a 30-min recovery period followed by the final sampling and measurement.

2.4. Chlorophyll fluorescence measurement and parameterization

A portable pulse amplitude modulated fluorometer (WATER-PAM, Walz, Germany) was used to determine chlorophyll fluorescence parameters. At each sampling point, the samples were dark adapted for 5 min first to relax photosynthetic activity (Gao et al., 2018a). The maximal efficiency of PSII photochemistry was defined as the ratio of variable to maximal chlorophyll fluorescence (F_V/F_M), where F_V = (F_M − F_0), F_M and F_0 were the maximal and minimal fluorescence yield, respectively. F_0 was measured by using modulated measuring light (< 0.1 μmol m^{-2} s^{-1}) and F_M was determined at a 0.5 s saturating pulse of 4000 μmol m^{-2} s^{-1}. F_V/F_M was used to estimate PSII activity since it

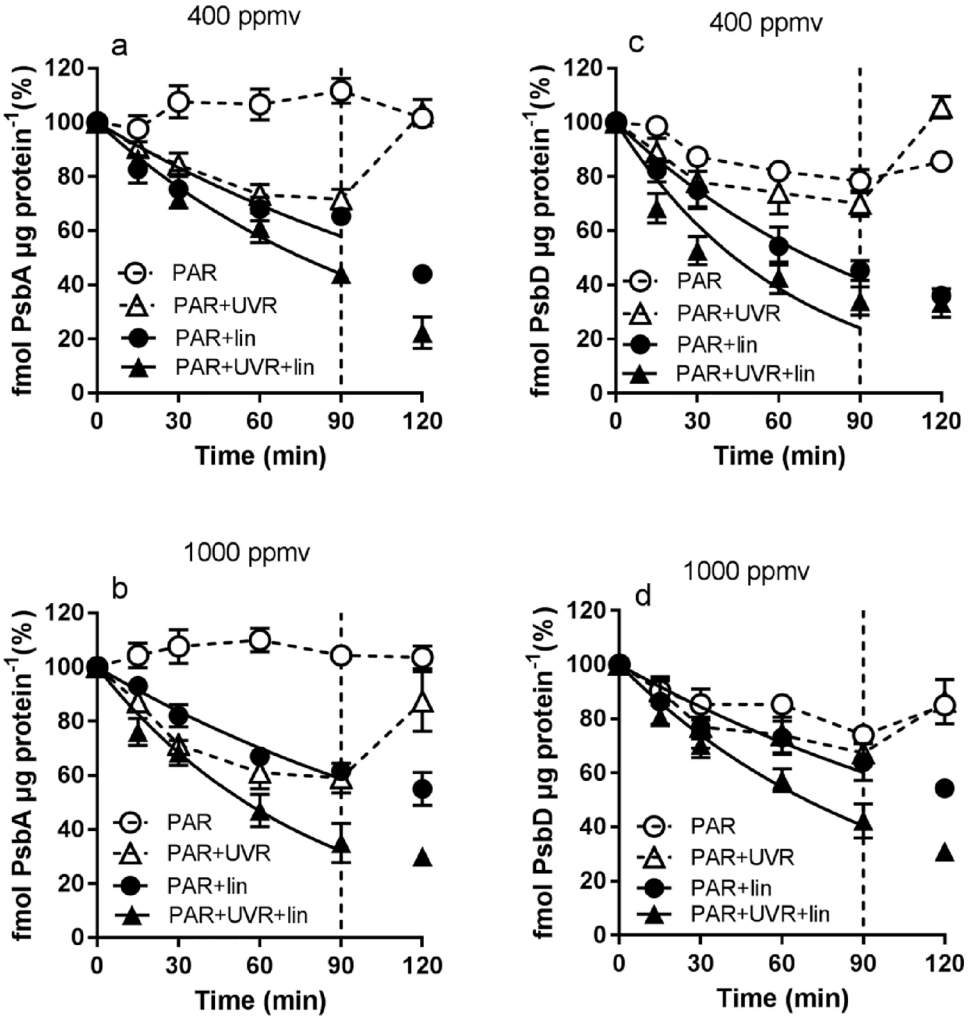

Fig. 2. Changes in PsbA (a, b) and PsbD (c, d) protein content in *T. weissflogii* cultures treated with (black symbols) or without (white symbols) the chloroplast protein synthesis inhibitor lincomycin. Cells were grown under two levels of CO_2 (400, 1000 ppmv) at the light intensity of 20 W m^{-2} PAR, then exposed to high radiation of PAR (140 W m^{-2}) or PAR (140 W m^{-2}) + UVR (26 W m^{-2}) for 90 min, and then allowed to recover at 20 W m^{-2} PAR for 30 min. The solid line shows the exponential decay fit of the PsbA and PsbD content in the lincomycin-treated samples versus time. The initial PsbA and PsbD were 86.7 ± 4.7 and 69.2 ± 5.1 fmol μg $protein^{-1}$ for cells grown at 400 ppmv CO_2, and 106.7 ± 9.6 and 74.1 ± 0.9 fmol μg $protein^{-1}$ for cells grown at 1000 ppmv CO_2. To analyse the effect of exposure time on F_V/F_M among different treatments, relative values (ratios of absolute to the initial values) were used here. Data are the means ± SE (n = 3).

Table 5
Multivariate analysis of variance for the effects of CO_2, UVR and limconmycin on PsbD and NPQs at different time points. CO_2*UVR means the interactive effect of CO_2 and UVR and the other terms with asterisk have similar meanings. df means degree of freedom, F means the value of F statistic, and Sig. means *p*-value.

Source	PsbD					NPQs				
	90 min			120 min		90 min			120 min	
	F	Sig.	df	F	Sig.	F	Sig.	df	F	Sig.
CO_2	2.104	0.166	1	0.104	0.752	7.155	0.013	1	0.434	0.516
UVR	12.119	0.003	1	0.141	0.712	21.384	< 0.001	1	0.379	0.544
Lincom	56.893	< 0.001	1	280.530	< 0.001	122.951	< 0.001	1	718.481	< 0.001
CO_2*UVR	0.395	0.539	1	10.032	0.006	1.563	0.223	1	0.599	0.446
CO_2*lincom	6.081	0.025	1	8.403	0.010	0.008	0.928	1	0.131	0.721
UVR*lincom	1.704	0.210	1	14.527	0.002	6.525	0.017	1	0.362	0.553
CO_2*UVR*lincom	0.757	0.397	1	0.026	0.874	0.121	0.731	1	0.008	0.927
Error			16					24		

is a rapid technique and the validation of using F_V/F_M to estimate active PSII in *T. pseudonana* has been done in our previous studies (Wu et al., 2012a).

The rate constant for photoinactivation (K_{pi}, s^{-1}) was calculated from lincomycin-treated samples by plotting a single phase exponential decay through a plot of F_V/F_M versus the cumulative photons applied during the high light treatment (Gao et al., 2018a). The rate constant for PSII repair (K_{rec}, s^{-1}) was calculated using non-lincomycin-treated samples (Gao et al., 2018a). Both calculations were made according to the Kok equation (Kok, 1956; Campbell and Tyystjärvi, 2012): $\frac{Y_t}{Y_0} = \frac{K_{rec}}{K_{pi}+K_{rec}} + \frac{K_{pi}}{K_{pi}+K_{rec}} e^{-(K_{pi}+K_{rec})t}$, where Y_0 and Y_t represent the maximal quantum yield at time zero and t (seconds), respectively.

A sustained phase of NPQ (NPQs), was defined as: NPQs = $(F_{Mt0}-F_M)/F_M$, where F_{Mt0} is the measurement of F_M from dark-acclimated cells, taken at time T_0 just before the start of high-light treatment and F_M is taken at each measurement time point after 5 min dark relaxation. By definition, NPQs thus starts from 0 at T_0, and increases if the cells accumulate a sustained phase of NPQ (Lavaud et al., 2004). NPQs reflects an inducible increase in the relaxation time for a fraction of NPQ, persisting beyond a 5-min dark period.

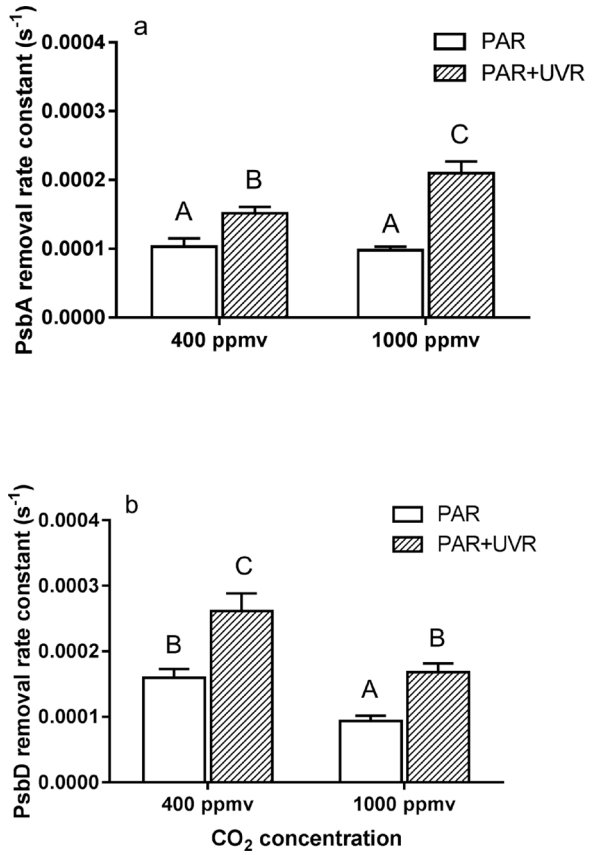

Fig. 3. PsbA (K_{PsbA}, s^{-1}) and PsbD (K_{PsbD}, s^{-1}) removal rate constant in *T. weissflogii* (a, b) grown under two levels of CO_2 (400, 1000 ppmv) with the light intensity of 20 W m^{-2} of PAR. Rate constants were estimated from the samples taken during 90 min of exposure to high PAR (140 W m^{-2}) or PAR (140 W m^{-2}) + UVR (26 W m^{-2}). Data are the means ± SE (n = 3). Different letters above error bars indicate significance differences (Tukey HSD, $P < 0.05$) among treatments.

Table 6
Two-way ANOVA for the effects of CO_2 and UVR on removal rate of PsbA and PsbD. CO_2*UVR means the interactive effect of CO_2 and UVR, df means degree of freedom, F means the value of F statistic, and Sig. means *p*-value.

Source	Removal rate of PsbA			Removal rate of PsbD		
	df	F	Sig.	df	F	Sig.
CO_2	1	3.876	0.085	1	16.580	0.004
UVR	1	35.727	< 0.001	1	20.512	0.002
CO_2*UVR	1	5.646	0.045	1	0.468	0.513
Error	8			8		

2.5. SDS-PAGE analysis and western blot

At each sampling point cells were harvested on glass fiber filters (25 mm diameter, binder-free glass fiber, Whatman), which were immediately flash frozen in liquid nitrogen and stored at −80 °C until later protein analyses. Total proteins were extracted by two thawing/sonicating rounds in denaturing extraction buffer (Brown et al., 2008). The total protein concentration was determined using a Lowry protein assay kit (Bio-Rad DC Assay). Western blots were performed for PsbA, PsbD and Rubisco large subunit (RbcL). Two μg of total protein was resolved by SDS polyacrylamide gel electrophoresis through 12% linear gradient polyacrylamide gel. Molar levels of PsbA (www.agrisera.se standard: AS01 017S) were then determined with quantitative immunoblotting (Wu et al., 2011).

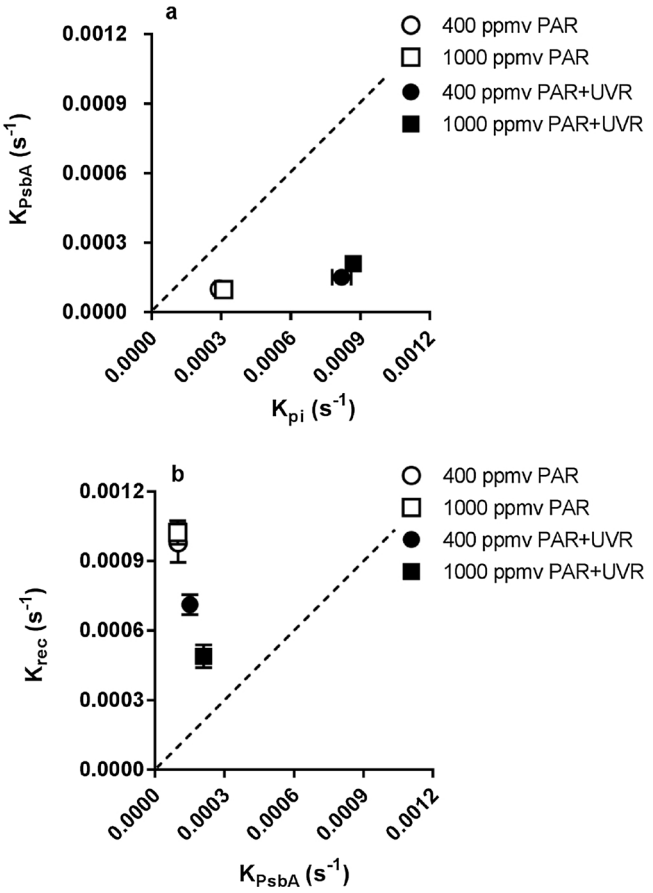

Fig. 4. PsbA removal rate constant (K_{PsbA}, s^{-1}) plotted versus photoinactivation rate constant (K_{pi}, s^{-1}) (a), and correlation of apparent PSII repair rate constant (K_{rec}, s^{-1}) and K_{PsbA} (s^{-1}) (b) for *T. weissflogii* grown under two levels of CO_2 (400, 1000 ppmv) with the light intensity of 20 W m^{-2} PAR. Rate constants were estimated from the samples taken during 90 min of exposure to high PAR (140 W m^{-2}) or PAR (140 W m^{-2}) + UVR (26 W m^{-2}). Dotted line indicates 1:1 ratio. Data are the means ± SE (n = 3 or 4).

We estimated a rate constant for the clearance of PsbA or PsbD protein by plotting fmol PsbA or PsbD μg total protein^{-1}, for cells incubated under the high light treatment in the presence of lincomycin to block the counteracting synthesis of PsbA or PsbD through chloroplast translation (Gao et al., 2018a). We fit this PsbA or PsbD plot with a single-phase exponential decay over the period from 0 to 90 min of high-light incubation. This K_{PsbA} or K_{PsbD} rate constant reflects the capacity for removal of PsbA or PsbD protein from the PSII pool (Wu et al., 2012a).

2.6. Statistical analysis

Results are expressed as means of replicates ± standard error. To assess the effect of exposure time on the parameters measured among various treatments, relative values (the ratios of absolute to initial values before the exposure) were used in some figures and the initial values were stated in figure legends. Data were statistically analysed using the software SPSS v.21. The data under every treatment conformed to a normal distribution (Shapiro-Wilk, $P > 0.05$) and the variances could be considered equal (Levene's test, $P > 0.05$). Multivariate Analysis of Variance (MANOVA) was conducted to assess the effects of CO_2 on carbonate parameters in cultures. Repeated measures Analysis of Variance (RM-ANOVA) was conducted to analyse the effect of exposure time on F_V/F_M, contents of PsbA, PsbD and Rubisco, NPQs, and ratio of RbcL to PsbA content. Bonferroni post-tests were conducted for *post hoc* investigation. Three-way MANOVA was

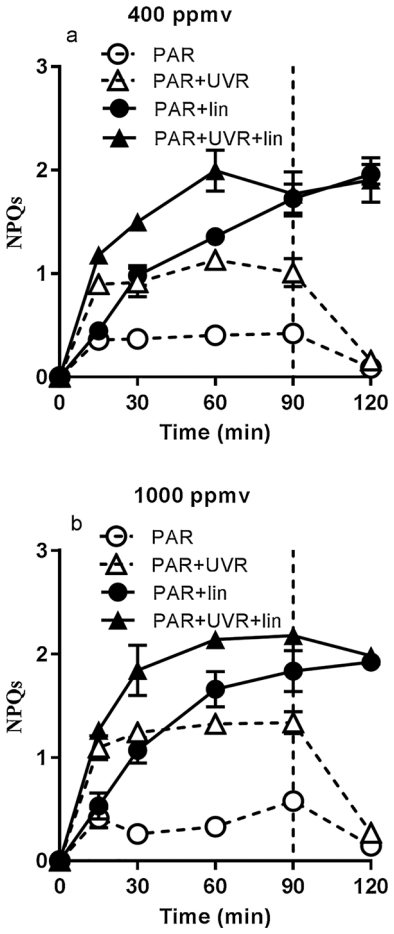

Fig. 5. Responses of sustained NPQ (NPQs) versus exposure time of high light in *T. weissflogii* cultures treated with (black symbols) or without (white symbols) the chloroplast protein synthesis inhibitor lincomycin. Cells grown under two levels of CO_2 (400, 1000 ppmv) with the light intensity of 20 W m^{-2} PAR were exposed to high radiation of PAR (140 W m^{-2}) or PAR (140 W m^{-2}) + UVR (26 W m^{-2}) for 90 min and then allowed to recover at 20 W m^{-2} PAR for 30 min. Data are the means ± SE (n = 4).

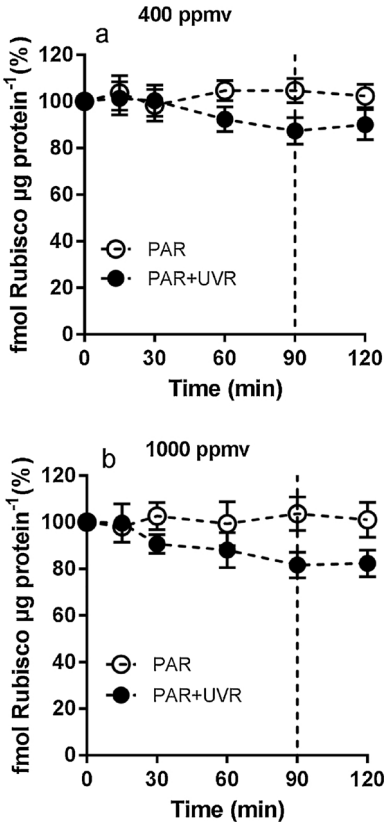

Fig. 6. Changes in Rubisco protein content in *T. weissflogii* cultures. Cells grown under two levels of CO_2 (400, 1000 ppmv) with the light intensity of 20 W m^{-2} PAR were exposed to high radiation of PAR (140 W m^{-2}) or PAR (140 W m^{-2}) + UVR (26 W m^{-2}) for 90 min and then allowed to recover at 20 W m^{-2} PAR for 30 min. The initial Rubisco content was 483.3 ± 33.3 and 360.0 ± 33.0 fmol µg $protein^{-1}$ for cells grown at 400 and 1000 ppmv CO_2 respectively. To analyse the effect of exposure time on F_V/F_M among different treatments, relative values (ratios of absolute to the initial values) were used here. Data are the means ± SE (n = 3).

used to analyse the effects of CO_2, UVR and lincomycin on F_V/F_M, contents of PsbA, PsbD and Rubisco, NPQs, and ratio of RbcL to PsbA at different exposure times. Two-way MANOVA was used to analyse the effects of CO_2 and UVR on Rubisco and ratio of RbcL to PsbA at different exposure times. Two-way ANOVA was used to analyse the effects of CO_2 and UVR on PsbA removal rates constant of PsbA and PsbD. Tukey HSD was conducted for *post hoc* investigation. Independent samples *t*-test was used to analyse the effects of CO_2 on content of PsbA, PsbD and Rubisco before light treatments. Significance was determined at $P < 0.05$ for all tests.

3. Results

The elevated CO_2 (air) altered carbonate parameters in seawater (Tables 1 & 2) and resulted in a decrease of 4.3% in pH and 50.2% in CO_3^{2-}, but an increase of 152.7% in pCO_2, 7.4% in DIC, 12.1% in HCO_3-, 152.7% in CO_2compared to 400 ppmv CO_2. Total alkalinity was not affected by CO_2.

The maximal photochemical efficiency (F_V/F_M) in *T. weissflogii* grown under all conditions decreased with exposure time when the cells were shifted from low light to high light (Fig. 1 & Table 3). Exposure time had an interactive effect with light treatment or lincomycin (Table 3). Specifically, cells exposed to PAR + UVR had a larger decrease in F_V/F_M compared to those exposed to PAR. F_V/F_M in cells without lincomycin treatment did not decrease further after 15 min of high light exposure but it decreased immediately with the addition of lincomycin during 90 min exposure. At the end of 90 min exposure, both UVR and CO_2 significantly reduced F_V/F_M (Table 4). For instance, UVR reduced F_V/F_M by 38.3% at 400 ppmv CO_2 and by 49.7% at 1000 ppmv CO_2, suggesting a higher decrease for the higher CO_2 condition. After the recovery at low light for 30 min, the F_V/F_M rose to 86.8–96.7% of the initial value in the absence of lincomycin, with cells treated by PAR + UVR or high CO_2 having slower recovery (Table 4). On the other hand, no recovery occurred when cells were incubated with lincomycin.

The higher CO_2 culture significantly enhanced the PsbA content (*t*

Table 7
Repeated analysis of variance for the effects of exposure time on Rubisco content and RbcL:PsbA under various conditions. Time*CO_2 means the interactive effect of exposure time and CO_2 and the other terms with asterisk have similar meanings. df means degree of freedom, F means the value of F statistic, and Sig. means *p*-value.

Source	Rubisco			RbcL:PsbA		
	df	F	Sig.	df	F	Sig.
Time	4	0.823	0.521	4	2.015	0.116
Time*CO_2	4	0.095	0.983	4	0.307	0.871
Time*UVR	4	2.056	0.110	4	3.488	0.018
Time*CO_2*UVR	4	0.362	0.834	4	0.273	0.893
Error	32			32		

Table 8
Multivariate analysis of variance for the effects of CO_2 and UVR on Rubisco and RbcL:PsbA at different time points. CO_2*UVR means the interactive effect of CO_2 and UVR, df means degree of freedom, F means the value of F statistic, and Sig. means *p*-value.

Source	Rubisco					RbcL:PsbA				
	90 min			120 min		90 min			120 min	
	F	Sig.	df	F	Sig.	F	Sig.	df	F	Sig.
CO_2	0.313	0.591	1	0.512	0.495	10.533	0.012	1	11.455	0.010
UVR	10.887	0.011	1	6.074	0.039	5.129	0.053	1	0.489	0.504
CO_2*UVR	0.153	0.706	1	0.254	0.628	0.041	0.844	1	0.323	0.585
Error			8					8		

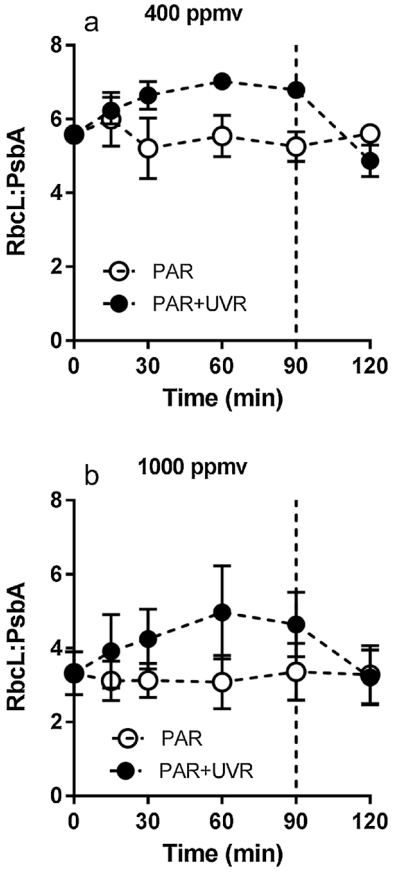

Fig. 7. Changes of the ratio of Rubisco large subunit (RbcL) to PsbA content in *T. weissflogii* cultures. Cells grown under two levels of CO_2 (400, 1000 ppmv) with the light intensity of 20 W m^{-2} PAR were exposed to high radiation of PAR (140 W m^{-2}) or PAR (140 W m^{-2}) + UVR (26 W m^{-2}) for 90 min and then allowed to recover at 20 W m^{-2} PAR for 30 min. Data are the means ± SE (n = 3).

(4) = −3.235, P = 0.032), leading to a higher initial value (86.7 ± 4.7 fmol μg protein^{-1} at 400 ppmv CO_2 and 106.7 ± 9.6 fmol μg protein^{-1} at 1000 ppmv CO_2) before the high light treatment. The change of PsbA content during the high light treatment was also monitored (Fig. 2a, b). After transferring to high light, exposure time had an interactive effect with UVR and lincomycin on the content of PsbA (Table 3). PsbA in cells exposed to PAR did not change during high light treatment but decreased in cells exposed to UVR with exposure time. With the addition of lincomycin, PsbA content decreased with exposure time irrespective of UVR or CO_2 treatments. At 90 min high light exposure, both UVRand CO_2 reduced PsbA content (Table 4). For instance, UVR reduced PsbA content by 35.8% at 400 ppmv CO_2 and 43.5% at 1000 ppmv CO_2. After 30 min recovery, PsbA content in cells without lincomycin increased to 87.3–103.7% of initial value. Lincomycin and UVR slowed down the recovery (Table 4).

The simulative effect of the higher CO_2 culture on the PsbD content (69.2 ± 5.1 fmol μg protein^{-1} at 400 ppmv CO_2 and 74.1 ± 0.9 fmol μg protein^{-1} at 1000 ppmv CO_2) was not statistically significant (t(4) = −1.645, P = 0.175). After transferring to high light, exposure time interplayed with UVR or lincomycin on content of PsbD protein (Fig. 2c, d and Table 3). Specifically, PsbD protein content decreased with the exposure time regardless of treatments. UVR or lincomycin led to a lower PsbD content. Contrary to PsbA, the exposure to PAR resulted in a significant decrease in PsbD. At 90 min high light exposure, lincomycin and UVR reduced PsbD content (Table 5).

In terms of removal rate of PsbA and PsbD protein (Fig. 3), UVR had a significant effect on PsbA removal rate and an interactive effect with CO_2 (Table 6). UVR increased PsbA removal rate under each CO_2 condition. The higher CO_2 did not affect PsbA removal rate under PAR but increased it under PAR + UVR. In contrast, higher CO_2 reduced PsbD removal rate regardless of UV treatment and UVR also enhanced PsbD removal rate (Table 6).

The K_{PsbA} (PsbA removal rate constant, based on the data in Fig. 3a) versus K_{pi} (photoinactivation rate constant, based on the data in Fig. 1) was plotted, for cells treated with lincomycin to block counteracting repair processes (Fig. 4a). Although PAR + UVR and CO_2 synergistically improved K_{PsbA} as shown in Fig. 3, it still lagged behind K_{pi}. The plot of K_{rec} (apparent PSII repair rate constant, based on the data in Fig. 1) versus K_{PsbA} (Fig. 4b) showed that functional recovery of PSII greatly exceeded K_{PsbA}. The stimulation of PAR + UVR on removal of PsbA, particularly under high CO_2, was not enough to catch up with apparent K_{rec}.

In terms of NPQs (Fig. 5), exposure time had a significant effect on NPQs and it interplayed with UVR or lincomycin (Table 3). NPQs increased after exposure to high light. UVR or the addition of lincomycin led to a bigger increase in NPQs. At the end of 90 min high light exposure, each factor significantly affected NPQs and UVR interacted with lincomycin (Table 5). *Post hoc* Tukey HSD comparison showed that higher CO_2, the presence of UVR and lincomycin induced higher NPQs and the inductive effect of UVR was more significant in the absence of lincomycin.

In addition to PSII, the combined effect of CO_2 and UVR on Rubisco content was also investigated (Fig. 6). The higher CO_2 culture significantly reduced the Rubisco content ($t_{(4)}$ = 4.557, P = 0.010), leading to a lower initial value (483.3 ± 33.3 fmol μg protein^{-1} at 400 ppmv CO_2 and 360.0 ± 33.0 fmol μg protein^{-1} at 1000 ppmv CO_2) before the high light treatment. Exposure time did not affect Rubisco content (Table 7). After 90 min high light exposure, CO_2 did not affect Rubisco content but UVR reduced it (Table 8). After 30 min low light recovery, Rubisco content under PAR + UVR was still lower than that under PAR (Table 8).

To analyse the effect of CO_2 and UVR on the relationship between light reaction and dark reaction of photosynthesis, the ratios of RbcL to PsbA under various treatments were calculated (Fig. 7). The exposure time and UVR had an interactive effect; that is, the ratio under PAR did not change with exposure time but that under PAR + UVR increased

with exposure time (Table 7). The higher CO_2 decreased the ratios at all time points regardless of radiation treatment while UVR did not affect the ratios (Table 8).

4. Discussion

High PAR exposure commonly reduces algal PSII activity, leading to photoinhibition (Neidhardt et al., 1998; Wu et al., 2012a; Havurinne and Tyystjärvi, 2017; Gao et al., 2018a). Photosynthetic organisms are more prone to be damaged by UVR and even very low dose of UVR could result in severe photoinhibition in diatoms (Gao et al., 2009; Wu et al., 2012b). In terms of the combined effect of increased CO_2 and UVR, it has been documented that they synergistically reduced the relative electron transport rate in the diatom *Cylindrotheca closterium* f. *minutissima* (Wu et al., 2012a) and increased photoinhibition of phytoplankton in Lake Giles, Pennsylvania (Sobrino et al., 2009). However, the potential reasons remain unknown. Our study also shows that the activity of PSII in *T. weissflogii* was significantly reduced during the exposure to PAR + UVR, and was accelerated in cells grown under high CO_2. This could be attributed to turnover rates of PsbA and PsbD during the PSII repair triggered by UVR and high CO_2.

The previous studies with model cyanobacteria, green algae and plants have shown that degradation of the PsbA protein is strictly light dependent, with rates exceeding those for other PSII proteins (Jansen et al., 1999; Komenda et al., 2012; Yao et al., 2012). For example, in *Synechocystis* PCC 6803, the PsbA proteins turn over ~5 × faster than the related PsbD protein (Yao et al., 2012). In contrast, as found in *Chaeotoceros gracilis* (Nagao et al., 2012), *Thalassiosira pseudonana* CCMP 1014 and *Coscinodiscus radiatus* CCMP 312 (Wu et al., 2011, 2012a), in *Thalassiosira pseudonana* CCMP 1335 (Campbell et al., 2013), and now the *Thalassiosira weissflogii* CCMA 102 (Fig. 3), the rate constant K_{PsbD} for removal of PsbD is comparable in magnitude to K_{PsbA} for removal of PsbA.

In this study, both PsbA and PsbD removal rate were stimulated by UVR. In case of PsbA repair after photodamage, the damaged PsbA protein need to be removed from the thylakoid membrane, and then the newly synthesized copy is reinserted (Komenda et al., 2012; Eaton-Rye and Sobotka, 2017). PsbD protein is hypothesized to act as a receptor component for newly synthesized PsbA protein, which is a key regulatory step for assembly of the PSII reaction center complex (Komenda et al., 2004). The removal of damaged PsbD and reinsertion of new synthesized PsbD might precede the reinsertion of PsbA during repair after PAR or UVR damage, thus this concerted repair mechanism could be in agreement with the enhanced PsbD protein turnover (Sass et al., 1997). However, different from PsbA, higher CO_2 reduced PsbD turnover rate in this study. The assembly of PSII reaction center complex was probably limited by the declination of PsbD removal under higher CO_2. Therefore, although the PsbA removal was synergistically increased by high CO_2 and UVR, the restoration of PSII photochemical activity was still retarded as shown in Fig. 1B.

UVR induced larger NPQs in *T. weissflogii* in this study, and this is consistent with the findings in *Phaeocystis globosa* (Chen and Gao, 2011) and *Gephyrocapsa oceanica* (Jin et al., 2013). NPQ is commonly considered a photoprotection mechanism that dissipates excess excitation energy in the form of heat (Goss and Jakob, 2010; Demmig-Adams et al., 2014). In diatoms, NPQ is dominated by one or more mechanisms activated by the trans-thylakoid proton gradient triggering the xanthophyll cycle (Lavaud et al., 2004; Lavaud and Lepetit, 2013). The increased NPQs under PAR + UVR may be related to UV-stimulated synthesis of xanthophyll pigments (Laurion and Roy, 2009). In addition to UVR, cells grown under the higher CO_2 condition showed higher NPQs during high light exposure in this study. High CO_2 can down-regulate CCMs in algae (Wu et al., 2012b; Xu et al., 2017; Gao et al., 2018b) and the saved energy combined together with UV radiation could lead to larger light stress and thus induce higher NPQ (Gao et al., 2012, 2016). However, the increased NPQs obviously did not offset the harm caused by the combination of high CO_2 and UVR, leading to noticeable photoinactivation. It is worth noting that NPQ is mostly related to xanthophyll cycle pigments that are not affected by lincomycin at most cases. Meanwhile, NPQ can be induced by photoinhibition (Serôdio and Lavaud, 2011; Gao et al., 2018a). Therefore, the higher NPQs in the presence of lincomycin may be due to photoinhibition that was enhanced by lincomycin.

It has been documented that the activity or amount of Rubisco protein in both higher plant and phytoplankton decreases after acclimation to elevated CO_2 concentrations (Drake et al., 1997; Tortell, 2000) because less Rubisco is required under elevated CO_2 for carbon fixation. We propose that the decrease in Rubisco expression under elevated CO_2 is a redistribution of nitrogen and could enhance the efficiency of nitrogen use. Our results support this hypothesis as more PsbA protein was synthesized with the decreased expression of Rubisco under the elevated CO_2 condition in this study. Accordingly more nitrogen can be used in defending high light and UVR challenge. The harmful effect of UVR on Rubisco has been seen in the previous studies (Keiller and Holmes, 2001; Takeuchi et al., 2002) and it has been attributed to active oxygen species induced by UV light (Hideg et al., 2000). Our study also shows that UVR reduced Rubisco content during 90 min exposure but it is worthy of noting that the harmful effect of UVR on Rubisco was much smaller than that on PSII, indicating that dark reaction is more tolerant to UVR compared to light reaction. In addition, the higher CO_2 decreased the ratio of RbcL to PsbA regardless of the radiation treatments, indicating that the carbon fixation capacity declined relative to the photochemical capacity for reductant generation, which also means that the capacity of cells to rapidly drain excess electrons in the Calvin cycle was lowered. This could also explain the higher inhibition of PSII photochemical activity for cells growing under the higher CO_2 condition during UVR exposure.

5. Conclusion

Our study, for the first time, demonstrates that increased CO_2 could deteriorate UVR-induced damage on PSII in the diatom *Thalassiosira weissflogii* through reducing PsbD removal rate and the ratio of RbcL to PsbA during UVR exposure. Although higher NPQ was induced and less Rubisco protein was expressed under increased CO_2 with more energy and materials flowing into the synthesis of PsbA and PsbD, it seemed not enough to counteract the negative effect from the combination of higher CO_2 and UVR, leading to increased harm on PSII function. Diatoms are deemed to be robust in dealing with fluctuating PAR and UVR, however, the increasing CO_2 and ocean acidification may impair their capacity in this aspect and thus affect their abundance and distribution in future ocean environment.

Author statement

Guang Gao: Conceptualization, Data analysis, Writing- Original draft preparation. Zhiguang Xu: Investigation, Writing- Reviewing and Editing. Qi Shi: Investigation. Hongyan Wu: Conceptualization, Data analysis, Writing- Reviewing and Editing, Supervision.

Acknowledgements

This research was supported by the National Natural Science Foundation of China (Nos. 31270452; 91647207; 41376129 and 41476097), the Research Project of Chinese Ministry of Education (No. 213026A), the Natural Science Foundation of Hubei Province (2014CFB607), the China Postdoctoral Science Foundation (2018T110463 & 2017M620270), Jiangsu Planned Projects for Postdoctoral Research Funds (1701003A) and the Priority Academic Program Development of Jiangsu Higher Education Institutions.

References

Bais, A.F., Mckenzie, R.L., Bernhard, G., Aucamp, P.J., Ilyas, M., Madronich, S., Tourpali, K., 2015. Ozone depletion and climate change: impacts on UV radiation. Photochem. Photobiol. Sci. 14, 19–52.

Biehler, K., 1996. Evidence for the contribution of the Mehler-Peroxidase reaction in dissipating excess electrons in drought-stressed wheat. Plant Physiol. 112, 265–272.

Boelen, P., Boer, M.D., Kraay, G.W., Veldhuis, M., Buma, A., 2000. UVBR-induced DNA damage in natural marine picoplankton assemblages in the tropical Atlantic Ocean. Mar. Ecol. Prog. Ser. 193, 1–9.

Boelen, P., van de Poll, W.H., van der Strate, H.J., Neven, I.A., Beardall, J., Buma, A.G., 2011. Neither elevated nor reduced CO_2 affects the photophysiological performance of the marine Antarctic diatom *Chaetoceros brevis*. J. Exp. Mar. Biol. Ecol. 406, 38–45.

Brown, C.M., MacKinnon, J.D., Cockshutt, A.M., Villareal, T.A., Campbell, D.A., 2008. Flux capacities and acclimation costs in *Trichodesmium* from the Gulf of Mexico. Mar. Biol. 154, 413–422.

Campbell, D.A., Tyystjärvi, E., 2012. Parameterization of photosystem II photoinactivation and repair. Biochimica et Biophysica Acta (BBA) – Bioenergetics 1817, 258–265.

Campbell, D.A., Hossain, Z., Cockshutt, A.M., Zhaxybayeva, O., Wu, H., Li, G., 2013. Photosystem II protein clearance and FtsH function in the diatom *Thalassiosira pseudonana*. Photosynth. Res. 115, 43–54.

Chen, S., Gao, K., 2011. Solar ultraviolet radiation and CO_2-induced ocean acidification interacts to influence the photosynthetic performance of the red tide alga *Phaeocystis globosa* (Prymnesiophyceae). Hydrobiologia 675, 105–117.

Demmig-Adams, B., Garab, G., Adams, W.W., Govindjee, 2014. Non-Photochemical Quenching and Energy Dissipation in Plants, Algae and Cyanobacteria. Springer, Netherlands.

Domingues, R.B., Guerra, C.C., Galvão, H.M., Brotas, V., Barbosa, A.B., 2017. Short-term interactive effects of ultraviolet radiation, carbon dioxide and nutrient enrichment on phytoplankton in a shallow coastal lagoon. Aquat. Ecol. 51, 91–105.

Drake, B.G., Gonzalez-Meler, M.A., Long, S.P., 1997. More efficient plants: a consequence of rising atmospheric CO_2? Annu. Rev. Plant Physiol. Plant Mol. Biol. 48, 609–639.

Dubinsky, Z., Stambler, N., MacIntyre, H., Berman, T., Frank, I.B., 2009. Photoacclimation processes in phytoplankton: mechanisms, consequences, and applications. Aquat. Microb. Ecol. 56, 163–176.

Eaton-Rye, J.J., Sobotka, R., 2017. Assembly of the photosystem II membrane-protein complex of oxygenic photosynthesis. Front. Plant Sci. 8, 884.

Falkowski, P., 2012. Ocean science: the power of plankton. Nature 483, 17–20.

Field, C.B., Behrenfeld, M.J., Randerson, J.T., Falkowski, P., 1998. Primary production of the biosphere: integrating terrestrial and oceanic components. Science 281, 237–240.

Gao, G., Gao, K., Giordano, M., 2009. Responses to solar UV radiation of the diatom *Skeletonema costatum* (Bacillariophyceae) grown at different Zn^{2+} concentrations. J. Phycol. 45, 119–129.

Gao, G., Liu, Y., Li, X., Feng, Z., Xu, J., 2016. An ocean acidification acclimatised green tide alga is robust to changes of seawater carbon chemistry but vulnerable to light stress. PLoS One 11, e0169040.

Gao, G., Shi, Q., Xu, Z., Xu, J., Campbell, D.A., Wu, H., 2018a. Global warming interacts with ocean acidification to alter PSII function and protection in the diatom *Thalassiosira weissflogii*. Environ. Exp. Bot. 147, 95–103.

Gao, G., Xia, J., Yu, J., Fan, J., Zeng, X., 2018b. Regulation of inorganic carbon acquisition in a red tide alga (*Skeletonema costatum*): the importance of phosphorus availability. Biogeosciences 15, 4871–4882.

Gao, K., Xu, J., Gao, G., Li, Y., Hutchins, D.A., Huang, B., Wang, L., Zheng, Y., Jin, P., Cai, X., 2012. Rising CO_2 and increased light exposure synergistically reduce marine primary productivity. Nat. Clim. Change 2, 519–523.

Gattuso, J.P., Magnan, A., Billé, R., Cheung, W.W.L., Howes, E.L., Joos, F., Allemand, D., Bopp, L., Cooley, S.R., Eakin, C.M., 2015. Contrasting futures for ocean and society from different anthropogenic CO_2 emissions scenarios. Science 349, 45–55.

Goss, R., Jakob, T., 2010. Regulation and function of xanthophyll cycle-dependent photoprotection in algae. Photosynth. Res. 106, 103–122.

Guillard, R.R., Ryther, J.H., 1962. Studies of marine planktonic diatoms. I. *Cyclotella nana* Hustedt, and *Detonula confervacea* (cleve) Gran. Can. J. Microbiol. 8, 229–239.

Häder, D.P., Kumar, H.D., Smith, R.C., Worrest, R.C., 2007. Effects of solar UV radiation on aquatic ecosystems and interactions with climate change. Photochem. Photobiol. Sci. 6, 267–285.

Häder, D.P., Williamson, C.E., Wängberg, S.Å., Rautio, M., Rose, K.C., Gao, K., Helbling, E.W., Sinha, R.P., Worrest, R., 2015. Effects of UV radiation on aquatic ecosystems and interactions with other environmental factors. Photochem. Photobiol. Sci. 14, 108–126.

Havurinne, V., Tyystjärvi, E., 2017. Action spectrum of photoinhibition in the diatom *Phaeodactylum tricornutum*. Plant Cell Physiol. 58, 2217–2225.

Hideg, E., Kálai, T., Hideg, K., Vass, I., 2000. Do oxidative stress conditions impairing photosynthesis in the light manifest as photoinhibition? Philos. Trans. R. Soc. B 355, 1511–1516.

Jansen, M., Mattoo, A., Edelman, M., 1999. D1-D2 protein degradation in the chloroplast. Complex light saturation kinetics. FEBS J. 260, 527–532.

Jin, P., Gao, K., Villafañe, V.E., Campbell, D.A., Helbling, E.W., 2013. Ocean acidification alters the photosynthetic responses of a coccolithophorid to fluctuating ultraviolet and visible radiation. Plant Physiol. 162, 2084–2094.

Keiller, D.R., Holmes, M.G., 2001. Effects of long-term exposure to elevated UV-B radiation on the photosynthetic performance of five broad-leaved tree species. Photosynth. Res. 67, 229–240.

Key, T., Mccarthy, A., Campbell, D.A., Six, C., Roy, S., Finkel, Z.V., 2010. Cell size trade-offs govern light exploitation strategies in marine phytoplankton. Environ. Microbiol. 12, 95–104.

Kim, J.-M., Lee, K., Shin, K., Kang, J.-H., Lee, H.-W., Kim, M., Jang, P.-G., Jang, M.-C., 2006. The effect of seawater CO_2 concentration on growth of a natural phytoplankton assemblage in a controlled mesocosm experiment. Limnol. Oceanogr. 51, 1629–1636.

Kok, B., 1956. On the inhibition of photosynthesis by intense light. Biochim. Biophys. Acta 21, 234–244.

Komenda, J., Reisinger, V., Müller, B.C., Dobáková, M., Granvogl, B., Eichacker, L.A., 2004. Accumulation of the D2 protein is a key regulatory step for assembly of the photosystem II reaction center complex in *Synechocystis* PCC 6803. J. Biol. Chem. 279, 48620–48629.

Komenda, J., Sobotka, R., Nixon, P.J., 2012. Assembling and maintaining the Photosystem II complex in chloroplasts and cyanobacteria. Curr. Opin. Plant Biol. 15, 245–251.

Landschützer, P., Gruber, N., Bakker, D.C.E., Schuster, U., 2015. Recent variability of the global ocean carbon sink. Glob. Biogeochem. Cycles 28, 927–949.

Laurion, I., Roy, S., 2009. Growth and photoprotection in three dinoflagellates (including two strains of *Alexandrium tamarense*) and one diatom exposed to four weeks of natural and enhanced ultraviolet-B radiation. J. Phycol. 45, 16–33.

Lavaud, J., Lepetit, B., 2013. An explanation for the inter-species variability of the photoprotective non-photochemical chlorophyll fluorescence quenching in diatoms. BBA Bioenergetics 1827, 294–302.

Lavaud, J., Rousseau, B., Etienne, A.L., 2004. General features of photoprotection by energy dissipation in planktonic diatoms (Bacillariophyceae). J. Phycol. 40, 130–137.

Li, G., Campbell, D.A., 2017. Interactive effects of nitrogen and light on growth rates and RUBISCO content of small and large centric diatoms. Photosynth. Res. 131, 93–103.

Macintyre, H.L., Kana, T.M., Geider, R.J., 2000. The effect of water motion on short-term rates of photosynthesis by marine phytoplankton. Trends Plant Sci. 5, 12–17.

Mackey, K.R., Morris, J.J., Morel, F.M., Kranz, S.A., 2015. Response of photosynthesis to ocean acidification. Oceanography 28, 74–91.

McCarthy, A., Rogers, S.P., Duffy, S.J., Campbell, D.A., 2012. Elevated carbon dioxide differentially alters the photophysiology of *Thalassiosira pseudonana* (Bacillariophyceae) and *Emiliania huxleyi* (Haptophyta). J. Phycol. 48, 635–646.

Moore, C.M., Mills, M.M., Arrigo, K.R., Bermanfrank, I., Bopp, L., Boyd, P.W., Galbraith, E.D., Geider, R.J., Guieu, C., Jaccard, S.L., 2013. Processes and patterns of oceanic nutrient limitation. Nat. Geosci. 6, 701–710.

Morel, F.M.M., Rueter, J.G., Anderson, D.M., Rrl, G., 1979. Aquil: a chemically defined phytoplankton culture medium for trace metal studies. J. Phycol. 15, 135–141.

Mostofa, K.M., 2016. Reviews and syntheses: ocean acidification and its potential impacts on marine ecosystems. Biogeosciences 13, 1767–1786.

Nagao, R., Tomo, T., Noguchi, E., Suzuki, T., Okumura, A., Narikawa, R., Enami, I., Ikeuchi, M., 2012. Proteases are associated with a minor fucoxanthin chlorophyll a/c-binding protein from the diatom, *Chaetoceros gracilis*. Biochim. Biophys. Acta 1817, 2110–2117.

Neidhardt, J., Benemann, J.R., Zhang, L., Melis, A., 1998. Photosystem-II repair and chloroplast recovery from irradiance stress: relationship between chronic photoinhibition, light-harvesting chlorophyll antenna size and photosynthetic productivity in *Dunaliella salina* (green algae). Photosynth. Res. 56, 175–184.

Newman, P.A., Mckenzie, R., 2011. UV impacts avoided by the Montreal Protocol. Photochem. Photobiol. Sci. 10, 1152.

Nixon, P.J., Michoux, F., Yu, J., Boehm, M., Komenda, J., 2010. Recent advances in understanding the assembly and repair of photosystem II. Ann. Bot. 106, 1–16.

Panel, U.N.E.P.E.E.A., 2017. Environmental effects of ozone depletion and its interactions with climate change: progress report, 2016. Photochem. Photobiol. Sci. 16, 107–145.

Pierrot, D., Lewis, E., Wallace, D.W.R., 2006. MS Excel Program Developed for CO_2 System Calculations. ORNL/CDIAC-105a. Carbon Dioxide Information Analysis Center, Oak Ridge National Laboratory, US Department of Energy, Oak Ridge, Tennessee.

Riebesell, U., Tortell, P.D., 2011. Effects of ocean acidification on pelagic organisms and ecosystems. In: Gattuso, J., Hansson, L. (Eds.), Ocean Acidification. Oxford University Press, Oxford, UK, pp. 99–121.

Sass, L., Spetea, C., Máté, Z., Nagy, F., Vass, I., 1997. Repair of UV-B induced damage of Photosystem II via de novo synthesis of the D1 and D2 reaction centre subunits in *Synechocystis* sp. PCC 6803. Photosynth. Res. 54, 55–62.

Serôdio, J., Lavaud, J., 2011. A model for describing the light response of the non-photochemical quenching of chlorophyll fluorescence. Photosynth. Res. 108, 61–76.

Six, C., Sherrard, R., Lionard, M., Roy, S., Campbell, D.A., 2009. Photosystem II and pigment dynamics among ecotypes of the green alga Ostreococcus. Plant Physiol. 151, 379–390.

Sobrino, C., Ward, M.L., Neale, P.J., 2008. Acclimation to elevated carbon dioxide and ultraviolet radiation in the diatom *Thalassiosira pseudonana*: effects on growth, photosynthesis, and spectral sensitivity of photoinhibition. Limnol. Oceanogr. 53, 350.

Sobrino, C., Neale, P.J., Phillips-Kress, J.D., Moeller, R.E., Porter, J.A., 2009. Elevated CO_2 increases sensitivity to ultraviolet radiation in lacustrine phytoplankton assemblages. Limnol. Oceanogr. 54, 2448–2459.

Solomon, S., Ivy, D.J., Kinnison, D., Mills, M.J., Rd, N.R., Schmidt, A., 2016. Emergence of healing in the Antarctic ozone layer. Science 353, 269–274.

Takeuchi, A., Yamaguchi, T., Hidema, J., Strid, A., Kumagai, T., 2002. Changes in synthesis and degradation of Rubisco and LHCII with leaf age in rice (*Oryza sativa* L.) growing under supplementary UV-B radiation. Plant Cell Environ. 25, 695–706.

Tortell, P.D., 2000. Evolutionary and ecological perspectives on carbon acquisition in phytoplankton. Limnol. Oceanogr. 45, 744–750.

Tyystjärvi, E., Aro, E.-M., 1996. The rate constant of photoinhibition, measured in lincomycin-treated leaves, is directly proportional to light intensity. Proc. Natl. Acad. Sci. U. S. A. 93, 2213–2218.

Wallington, T.J., Schneider, W.F., Worsnop, D.R., Nielsen, O.J., Sehested, J., Debruyn, W.J., Shorter, J.A., 1994. The environmental impact of CFC replacements HFCs and HCFCs. Environ. Sci. Technol. 28, 320A–326A.

Wu, H., Cockshutt, A.M., Mccarthy, A., Campbell, D.A., 2011. Distinctive photosystem II photoinactivation and protein dynamics in marine diatoms. Plant Physiol. 156, 2184–2195.
Wu, H., Roy, S., Alami, M., Green, B.R., Campbell, D.A., 2012a. Photosystem II photoinactivation, repair, and protection in marine centric diatoms. Plant Physiol. 160, 464–476.
Wu, X., Gao, G., Giordano, M., Gao, K., 2012b. Growth and photosynthesis of a diatom grown under elevated CO_2 in the presence of solar UV radiation. Fund. Appl. Limnol. 180, 279–290.
Xu, Z., Gao, G., Xu, J., Wu, H., 2017. Physiological response of a golden tide alga (*Sargassum muticum*) to the interaction of ocean acidification and phosphorus enrichment. Biogeosciences 14, 671–681.
Yao, D.C., Brune, D.C., Vermaas, W.F., 2012. Lifetimes of photosystem I and II proteins in the cyanobacterium *Synechocystis* sp. PCC 6803. FEBS Lett. 586, 169–173.
Yin, R., Ulm, R., 2017. How plants cope with UV-B: from perception to response. Curr. Opin. Plant Biol. 37, 42–48.
Young, J.N., Morel, F.M.M., 2015. Biological oceanography: the CO_2 switch in diatoms. Nat. Clim. Change 5, 722–723.